An In-Situ Interdiffusion Method for Harvesting Energy from an Aluminum-Water Reaction

by

Erich John Brandeau

Submitted to the Department of Mechanical Engineering
in partial fulfillment of the requirements for the degree of

Bachelor of Science in Mechanical Engineering

at the

MASSACHUSETTS INSTITUTE OF TECHNOLOGY

June 2012

Author .....
Department of Mechanical Engineering
May 25, 2012

Certified by .....
Douglas P. Hart
Professor of Mechanical Engineering
Thesis Supervisor

Accepted by .....
John H. Lienhard V
Samuel C. Collins Professor of Mechanical Engineering
Associate Department Head, Education

An In-Situ Interdiffusion Method for Harvesting Energy from an Aluminum-Water Reaction

by

Erich John Brandeau

Submitted to the Department of Mechanical Engineering
on May 25, 2012, in partial fulfillment of the
requirements for the degree of
Bachelor of Science in Mechanical Engineering

Abstract

Autonomous underwater vehicles (AUVs) are indispensable for countless underwater tasks but are currently limited in their range and endurance by the energy density of their battery packs. Aluminum is an ideal energy source for AUVs because it exothermically reacts with water and is two orders of magnitude more energy dense than current lithium-ion batteries. An in-situ interdiffusion method for reacting aluminum in water was conceived in which elemental aluminum is able to overcome the passivating aluminum oxide layer by diffusing into liquid gallium. The aluminum atoms in solution with the gallium react to produce heat and hydrogen gas when they reach the interface of the liquid gallium and water. This thesis attempts to quantify the diffusion of aluminum into liquid gallium as well as to quantify the reaction of the aluminum-gallium solution in water. Experiments are conducted to measure the diffusion and reaction rate constants, and the data is fit to the Arrhenius equation to predict the diffusion and reaction rates at elevated system temperatures. With the predicted diffusion and reaction rates, it was found how the size and temperature effect the power output of an in-situ inderdiffusion aluminum-water reactor.

Thesis Supervisor: Douglas P. Hart
Title: Professor of Mechanical Engineering

Acknowledgements

Most importantly I must thank the 'Galinstan' team at MIT which consists of Ian McKay, Ruaridh Macdonald, Latifah Hamzah, Julian Merrick, and Winston Larson. They willingly allowed me to stick my nose in the project and have provided invaluable help with the theory, experiments, and ideas. Without this group of undergraduates, this project most definitely would not exist.

I would like to thank my advisor, Doug Hart, for encouraging our work and giving up lab space for our experiments. His confidence in this project was inspiring.

Nick Pulsone and his team at Lincoln Laboratory deserve credit for their enthusiasm in the project and their work in earning funding.

I would like to thank Tess Saxton-Fox and Keith Durand for their support.

Lastly, I thank my family and friends for supporting me on my undergraduate journey. I have definitely come a long way in the last four years.

Contents

List of Figures

List of Tables

Nomenclature

c instantaneous concentration of aluminum in gallium [wt%]

c'_{diff} diffusion rate $[\frac{\text{mg}}{\text{cm}^2\text{s}}]$

c'_{rxn} reaction rate $[\frac{\text{mg}}{\text{cm}^2\text{s}}]$

c_0 saturation concentration of aluminum in gallium [wt%]

E_a activation energy $[\frac{J}{mol}]$

k_{diff} diffusion rate constant $[\frac{\text{mg}}{\text{cm}^2\text{s}}]$

k_{rxn} reaction rate constant $[\frac{\text{mg}}{\text{cm}^2\text{s}}]$

P power [W]

R universal gas constant $[\frac{\text{J}}{\text{mol}\cdot\text{K}}]$

SA surface area

T temperature [K]

t time [s]

Al elemental aluminum

Ga elemental gallium

wt% weight percent

Chapter 1

Introduction

Generating power in underwater environments where oxygen is limited has proven to be a technological problem that has yet to be solved. Aluminum reacts in seawater with more than twice the energy density by volume of diesel burning in air, but to-date there are no underwater power sources that use aluminum as a fuel. An aluminum reaction engine that satisfies the power requirements of underwater vehicles could revolutionize the use of robotic vehicles in exploring and monitoring the 70% of the Earth that is covered in water.

1.1 Autonomous Underwater Vehicles

The development of unmanned submersible vehicles has recently been an important topic in the maritime community. Autonomous underwater vehicles (AUVs) have proven valuable for a variety of different uses, including ocean monitoring, seafloor mapping, search and rescue, ship and oil rig inspection and military operations, to name a few. An AUV mapping the seafloor is illustrated in Figure 1.1.1. Many attributes have made AUVs desirable for underwater applications. AUVs are much less expensive to design, build and operate than manned vessels, and often have much greater capability. The decreased cost allows AUVs to undertake missions that would otherwise be too costly, and because AUVs are unmanned, they can conduct missions that are otherwise too hazardous for a manned vehicle.

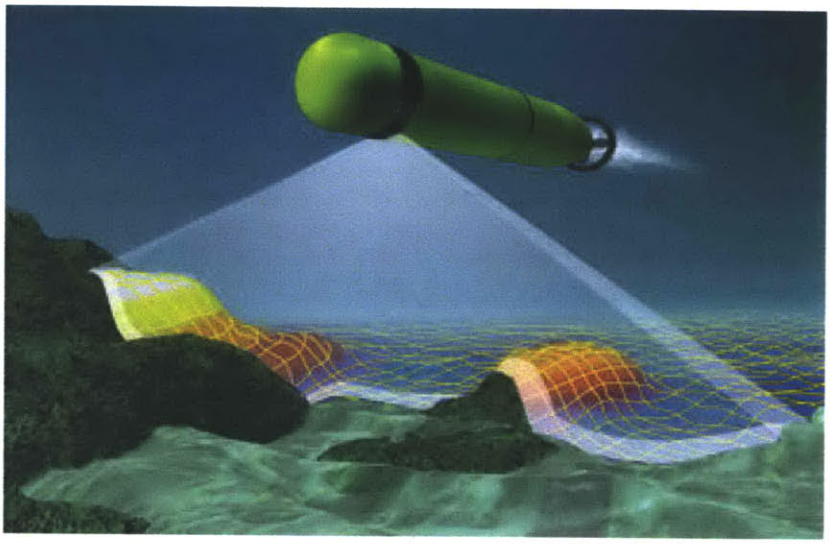

Figure 1.1.1: An artist's rendition of an AUV using sonar to map the ocean floor.

Currently, batteries are used to store energy in AUVs. For propulsion, two different systems are used: propeller driven or buoyancy driven. Buoyancy driven AUVs use the vertical motion of the vehicle to provide horizontal force through a hydrofoil. These AUVs operate slowly and must use the ocean currents to their advantage. A research glider built by researchers at Rutgers University crossed the Atlantic Ocean traveling east in a total of 221 days averaging roughly 0.5 knots on the way [1]. The entire journey consumed approximately 28 MJ of energy. The slow speed of these buoyancy driven vehicles makes them impractical for many uses, especially considering that ocean currents in some places can top 0.5 knots, which greatly inhibits the capability of these ocean gliders. Propeller driven AUVs can move much faster but are less efficient. The Hydroid REMUS 600 is a single propeller driven AUV that has a top speed of roughly 5 knots. It operates on a 15 kWh (54 MJ) lithium-ion battery pack and has a standard endurance of 70 hours before the vehicle must be recharged [2]. Vehicles like the REMUS 600 are commonly used for ocean exploration and Navy operations because of their speed and sensor capability.

Because of the limitations of AUV endurance, surface vessels must remain close to the AUVs in order to retrieve and recharge them every few days. The cost of operating

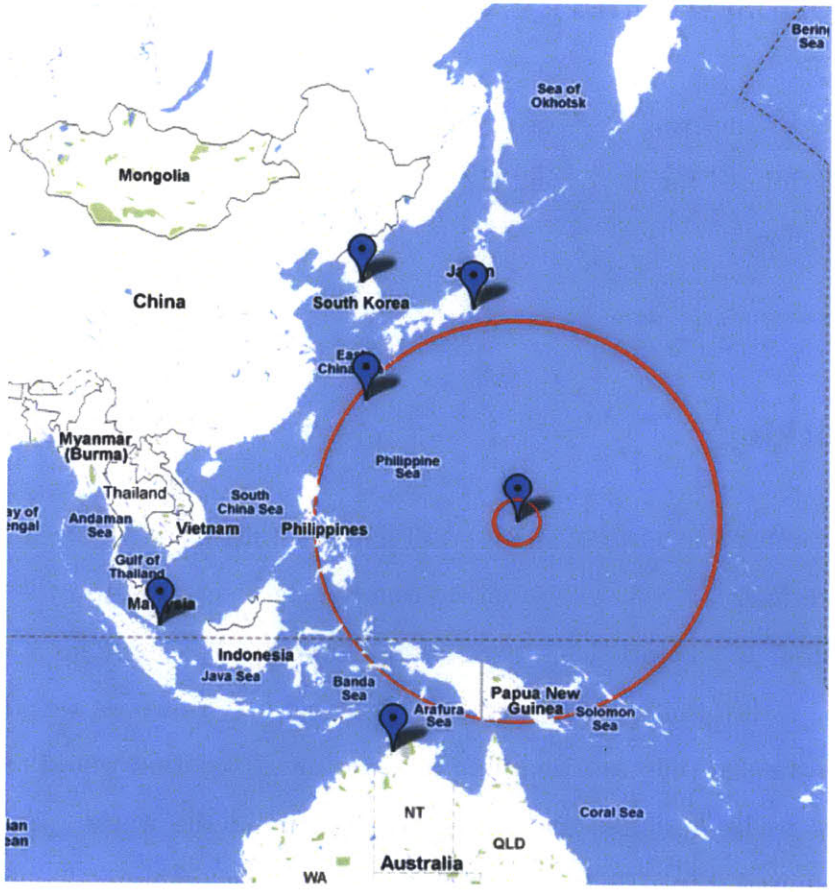

Figure 1.1.2: Current and desired range of AUVs. The inner circle is the current range of the REMUS 600 and the outer circle is the desired range. The points mark select Navy bases in the Pacific Ocean.

the surface vessels quickly surpasses the cost of the AUVs, and this currently prohibits their widespread use. If an order of magnitude more energy storage were available in a vehicle such as the REMUS 600, the practicality of the vehicle would be greatly increased. The AUV would be able to continue autonomously for nearly a month before needing to be refueled. To illustrate the importance of extended range, Figure 1.1.2 shows the current range of a REMUS 600 and the hypothetical range of a REMUS 600 with ten times the energy capacity. For reference, the center of the range is located at a United States Naval Base in the Pacific Ocean. With improved energy capacity, it is clear that AUVs would become much more practical and would require less interference from surface vessels.

1.2 Proposed Energy Sources

As part of the Engineering Systems Design class at MIT in the Fall of 2011, multiple ideas were considered for increasing the energy capacity of an AUV. These ideas are summarized below.

1.2.1 Docking

The docking concept consists of an external power supply from which the AUV's batteries could recharge. Such system have already been demonstrated to be successful [3]. The system is advantageous because it eliminates the need for a complicated power system within the space constraints of the vehicle. However, docking is a relatively small-scale solution, and enabling ocean-wide exploration would require a vast infrastructure to be designed and implemented around the world. Because of the additional required infrastructure of docking systems, self-contained energy capacity is highly desired for ocean-going AUVs.

1.2.2 Renewable Energy

Harvesting wind, solar, or wave energy was another concept considered for the recharging of an AUV. Solar-powered AUVs are currently being developed and have proven successful in long endurance operations [4]. Hypothetically, a solar-powered AUV could remain deployed for long periods of time with no human intervention. However, it was determined that these sources of energy did not have a great enough power density for the recharging of an AUV such as the REMUS 600 which has a cruising speed of 2.5 knots and is used for many different types of missions. With such a system, the vehicle would take too long to recharge and would become impractical to use.

1.2.3 Internal Reactions

There exist many fuels which could be carried by the AUV and reacted to produce energy. Many of the common fuel sources are highlighted in Figure 1.2.1. Hydrocarbons were considered as a good option for additional energy storage because of their widespread use and established technology. However, a vehicle which burns hydrocarbons in order to recharge the batteries must do so at the surface of the water such that air can be snorkeled into the vehicle for the combustion. If oxygen is brought along with the vehicle, the energy density of the system decreases to the energy density of lithium-ion batteries, so no improvement is made. Therefore, a fuel that reacts in water, rather than air, is desired because it would enable the AUV to burn the fuel at depth. In this manner energy could be constantly produced, so the required power output of the energy source is much less than if the energy was produced intermittently. Fuels that react in water, including sodium and aluminum, were identified and investigated. Sodium, which reacts violently in water, has roughly half the energy density of most hydrocarbons. It is also a fairly hazardous element to handle. On the contrary, aluminum has one of the highest energy densities of common fuel sources, and is also very safe. For these reasons, aluminum was pursued as a highly desirable source of energy for underwater vehicles.

1.3 Thesis Summary

This thesis presents an in-situ interdiffusion method for harvesting energy from an aluminum-water reaction and predicts the power output as a function of reactor size and temperature. The use of aluminum as a fuel source is discussed in Chapter 2. The in-situ interdiffusion method is discussed in Chapter 3. The experiments to characterize the temperature and concentration dependence of the method are discussed in Chapter 4. Finally, the power output of the reaction as a function of reactor design parameters is given in Chapter 5.

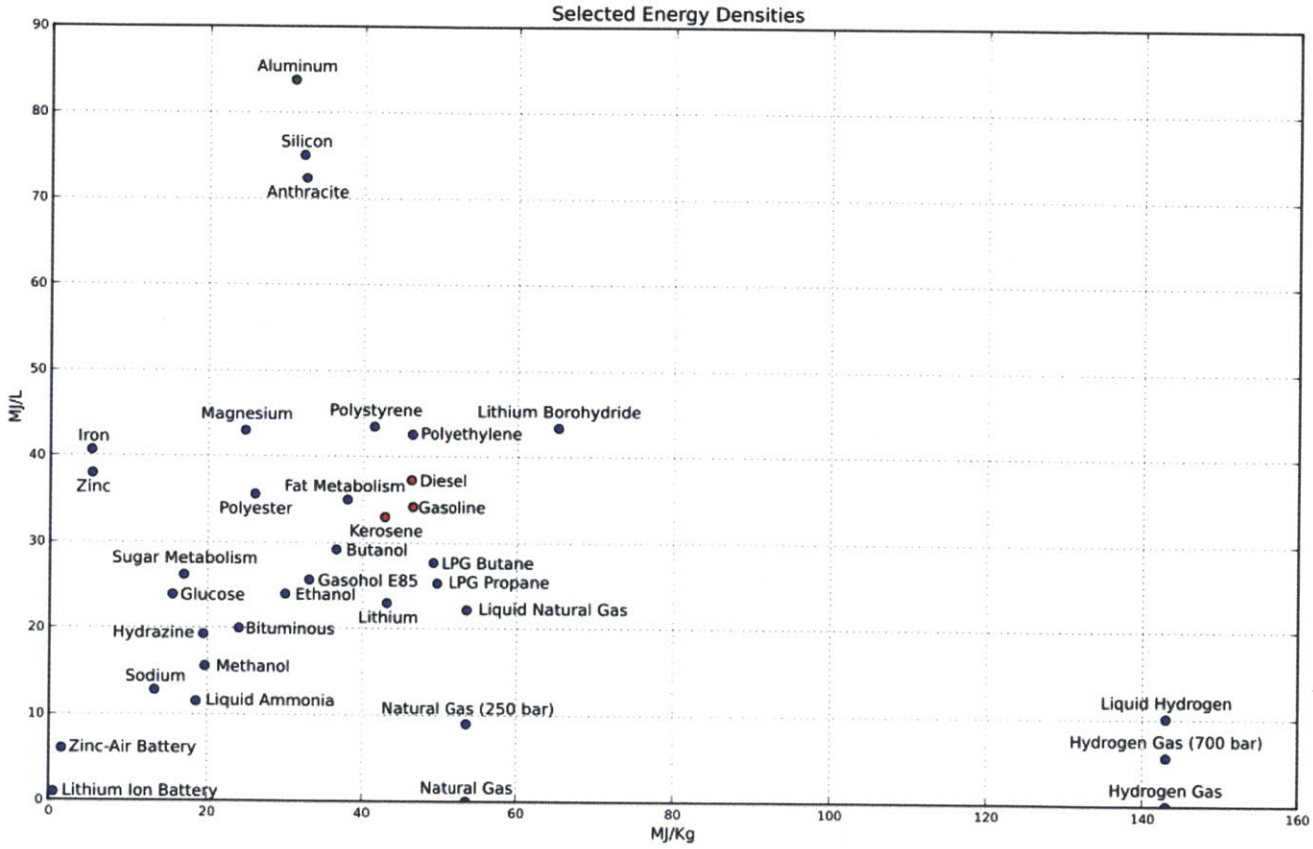

Figure 1.2.1: Energy densities of common fuel sources, disregarding mass of reactants.

Chapter 2

Aluminum as a Fuel Source

It has long been known that pure aluminum reacts in water by oxidizing with the oxygen from the H_20 molecule. Normally, the reaction is prohibited by the very thin passivation layer of aluminum oxide (Al_2O_3) that forms on the surface. In order to react the aluminum, the passivation layer must be disrupted. Many different methods have been considered; these approaches will be outlined below.

2.1 Background

At room temperature, water and aluminum produce aluminum hydroxide and hydrogen in an exothermic reaction.

$$2Al + 6H_2O \rightarrow 2Al(OH)_3 + 3H_2 + Q \tag{2.1.1}$$

The reaction is thermodynamically favorable over many temperatures, as shown in Table 2.1.1, and is highly exothermic. Using the Gibb's free energy from Table 2.1.1, the reaction releases 15.89 MJ/kg Al, or 4.414 kWh/kg Al of heat at a reaction temperature of 100° C. With an aluminum density of 2.7 kg/L, that equates to 42.9 MJ or 11.92 kWh per liter of aluminum of heat energy. For comparison, 38.5 MJ of energy is released per liter of diesel fuel combusted in air.

If the hydrogen gas produced by the reaction is burned, additional energy can also

Temp (C)	$\triangle H$ (kJ/mol H2)	$\triangle S$ (J/K)	$\triangle G$ (kJ/mol H2)
0	-277	26.2	-284
100	-284	3.29	-286
200	-291	-12.1	-285
300	-298	-25.1	-283
400	-306	-38.0	-280
500	-316	-51.8	-276
600	-328	-66.8	-270

Table 2.1.1: Thermodynamics of the aluminum-water reaction. [5]

be released, and is given by the chemical equation,

$$2H_2 + O_2 \rightarrow 2H_2O + 572\text{kJ}. \tag{2.1.2}$$

For every liter of aluminum reacted in water, there is an additional 42.9 MJ of energy available from the combustion of the hydrogen. Using the hydrogen as an additional source of energy would double the energy output of the aluminum fuel; however, for this thesis, the additional energy from the hydrogen is ignored and all of the power calculations incorporate only the heat energy.

2.2 Prior Work

Aluminum has been long known as a fuel source but previous attempts to react aluminum with water have had mixed success.

A 2002 paper from the Applied Research Laboratory at Pennsylvania State University proposes a hypothetical AUV energy system based on aluminum-seawater combustion [6]. The basic concept of the approach is to feed aluminum powder into a high temperature high pressure chamber where it melts and oxidizes with water. The high temperature outlet is fed to a turbine and is used to drive the Rankine cycle. Because of the high temperatures (800-1100° C), a significant amount of oxide is produced in an environment of supercritical water. The group presents a method and

device for separating the large amount of oxide from the working fluid. The paper is largely based on theory, and currently an entire working system has yet to be shown.

A U.S. Department of Energy (DOE) white paper, "Reaction of Aluminum with Water to Produce Hydrogen" (2008), is a thorough survey of the field at the time of publication, but the paper was considering the aluminum-water reaction only as a source of hydrogen for hydrogen-powered land vehicles [5]. The paper concludes that the hydrogen output of the reaction does not meet the 2010 DOE system targets for highway vehicles and is an order of magnitude more expensive than the DOE target for hydrogen cost. The paper outlines hydroxide promoters, oxide promoters, salt promoters, aluminum pretreatment and molten aluminum alloys as reaction-promoting approaches. However, because the focus is hydrogen production, the paper ignores the heat produced by the reaction.

The DOE paper highlights Professor Jerry Woodall's research at Purdue University using aluminum-gallium alloys to produce hydrogen. The Purdue approach creates a high aluminum-content two-phase alloy using gallium, Ga-In-Sn or some other low melting temperature metal. The approach requires manufacturing a mechanically solid alloy which will then react in water. A 2010 doctoral thesis by Jeffrey Ziebarth describes the work done at Purdue to characterize the storage and conversion of energy using an Al-Ga-In-Sn alloy [7]. The work done by the Purdue group led to the creation of AlGalCo LLC, a company that is commercializing the use of an aluminum-gallium alloy to generate electricity. [8]

In order to understand the approach of the Purdue group, a similar experiment was created in the lab. An alloy of 50wt% aluminum-50wt% gallium was made in a nitrogen-purged furnace and then reacted in water. The metal reacted for a period of time but soon became coated in the hydroxide product, which appeared dark and muddy. After a while, the reaction stopped completely and a solid piece of material still remained. The hydroxide products also contained waste gallium because the gallium is not reacted with the aluminum. Because gallium is by far the most expensive part of the fuel, separating the gallium for reuse is desirable, yet proved to be a challenge.

The approach presented by Ziebarth was identified as having a few problems: 1) The reaction was choked by the hydroxide product and was unable to proceed to completion in an environment of only water. 2) The recovery of the gallium from the hydroxide products was difficult and would likely require additional systems. 3) The solid alloy fuel has to be made in a specific way in a furnace which further increases the expense of the fuel. 4) The solid fuel alloy has to be handled with care because any contact with water will trigger the reaction. On a large scale, the proper handling and transportation of the fuel would also further increase the expense and complexity of the fuel. Because of these problems, the in-situ diffusion method presented in this thesis was developed.

Chapter 3

In-Situ Diffusion Reactor Concept

3.1 Overview

The basic concept outlined in this thesis, unlike the methods described before, is to react aluminum with water by diffusing the aluminum in-situ through a liquid gallium interface. (Figure 3.1.1) The aluminum has a naturally-forming passivation layer protecting it from reacting, but when the aluminum is in contact with gallium, the interdiffusion potential of the two elements overcomes the passivation layer and brings elemental aluminum in solution with the liquid gallium. When the aluminum atoms reach the gallium/water boundary, they react with the water and release heat and hydrogen. The aluminum hydroxide products are left suspended in the water.

3.2 Advantages over Previous Methods

There are a few main advantages to the proposed in-situ diffusion approach: 1) the reaction products do not stick to the surface of the fuel because it is in liquid phase, so the reaction doesn't get choked off and is able to continue to completion. 2) The fuel is pure aluminum (or aluminum alloy), and requires no special handling or processes to make (i.e. no alloying with other metals). 3) The gallium remains in the reactor,

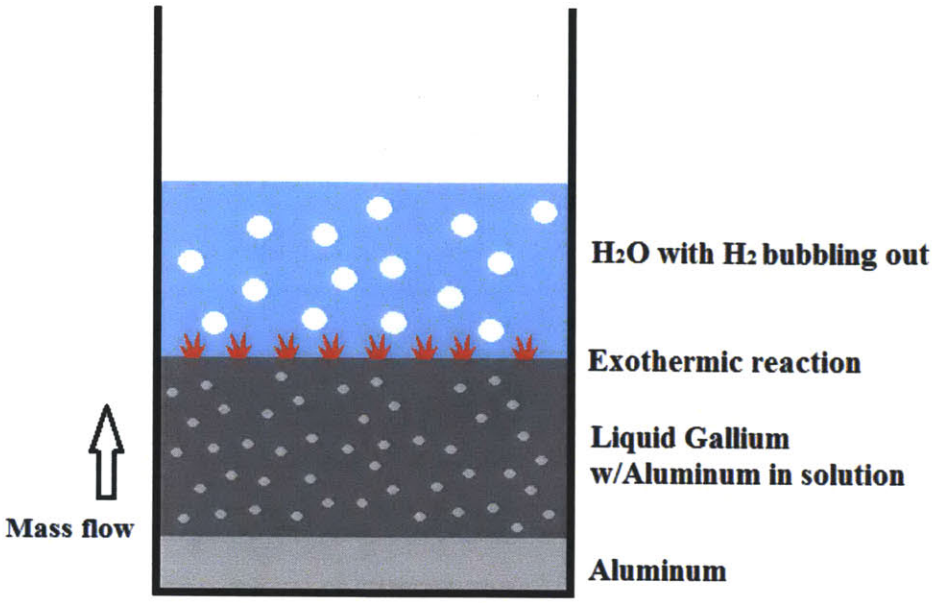

Figure 3.1.1: Schematic of basic in-situ diffusion concept.

and is not a part of the fuel. By localizing the gallium in the system and using it only as an in-situ aluminum transport mechanism, the overall required gallium is reduced and the complexity of recovering the gallium from the reaction products is eliminated.

3.3 Initial Observations and Hypothesis

Initially, the diffusion and reaction were conducted separately in order to analyze each independently. The solution was created by submerging thin aluminum wire in liquid gallium and allowing the diffusion to occur. After a few hours, the aluminum wire was substantially more brittle and the remaining liquid was reactive in water. The solution was also visibly more oxidized in air than pure gallium. The brittle aluminum was expected and is a result of the gallium diffusing into the grain boundaries of the aluminum which disrupts the crystal structure and compromises the strength of the material [9]. When a small amount of aluminum was used, especially as foil, it was observed that the aluminum would completely disappear into the gallium such that the solution was entirely liquid.

While the diffusion took a few hours, the reaction lasted for no more than 20 minutes. Upon dropping the liquid metal into water, the reaction started instantly and produced visible hydrogen bubbles. The liquid metal is immiscible in water so it remains intact in the water. It was observed that if initially solid metal was dropped in warm water, the reaction products were black in color and not very soluble in water. Once the metal became liquid, the reaction products were light in color and appeared powdery, making a cloudy colloidal solution in the water. If a small liquid sample of metal was dropped in a large amount of cold water, however, the reaction would begin but stop as soon as the metal froze because the heat generated was not enough to be self-sustaining.

After reacting, the liquid metal appears the same as before the reaction, but is inert in water. The reacted metal appears to be pure gallium, and is able to absorb more aluminum and react it without any loss in performance.

In order to work as a power source, however, it was clear that the diffusion rate would have to be maximized and matched with the reaction rate, such that the aluminum transfer into the gallium was the same as the aluminum transfer out of the gallium. Chapters 4 and 5 discuss the work that was done to characterize the diffusion and reaction rates in order to realize a possible design for an in-situ diffusion reactor of the concept shown in Figure 3.1.1.

Chapter 4

Experiments and Observations

4.1 Overview

Experiments were conducted on both the diffusion and reaction of aluminum in gallium in order to understand their rate dependence on temperature and aluminum concentration. Because the diffusion experiments involved reacting the aluminum out of the gallium, the diffusion and reaction experiments are closely linked and dependent on each other. The experimental techniques will be outlined, as well as the experiments conducted in order to prove assumptions and validate experiments.

4.2 Measuring Aluminum Concentration in Gallium

In order to analyze the characteristics of the diffusion, the aluminum concentration in the gallium must be measured. Because the saturation concentration of aluminum in liquid gallium is low ($\approx$1 wt%), it is challenging to directly measure the concentration of the solution. Density measurements require more sensitive volume measurements than could be taken with the instruments in the lab. So, the aluminum concentration is measured by reacting the sample and collecting the hydrogen gas. The volume of hydrogen gas is directly proportional to the aluminum mass present in the sample.

At atmospheric pressure of hydrogen, aluminum content is given by

$$1\text{mL}, H_2 \cdot \frac{1\text{L}}{1000\text{mL}} \cdot \frac{1\text{mol}}{22.378\text{L}} \cdot \frac{2\text{mol}, \text{Al}}{3\text{mol}, H_2} \cdot \frac{27\text{g}}{1\text{mol}, \text{Al}} = 8.044 \times 10^{-4} \frac{\text{g}, \text{Al}}{\text{mL}, H_2}, \quad (4.2.1)$$

which is derived from the chemical equation given by Equation 2.1.1 and the density of hydrogen gas. Given an initial sample mass and the hydrogen gas yield, the aluminum concentration in the sample can be determined. This experiment, however, relies on the assumption that the aluminum-gallium alloy reacts to completion. In order to verify the validity of this assumption, XRD was conducted on a reacted sample.

4.2.1 X-Ray Crystallography Results

In order to prove the assumptions about the reaction proceeding to completion, X-Ray diffraction (XRD) was performed on a sample of reacted liquid alloy. A small drop of the metal was frozen and then analyzed. The analysis of the data was done using PANalytical HighScore Plus [10]. The raw data of this analysis is shown in Figure 4.2.1, and the gallium reference peaks are overlayed for reference. The large peak around 36° was determined to be an artifact of the test because the beam width was greater than the sample width, so the sample platform registered as an intense peak. The analysis software showed no significant matches for aluminum in the sample, which gives reasonable evidence that the reacted metal is almost entirely gallium. In order to quantify the content of the reacted metal, however, more extensive crystallography should be performed.

The solid reaction products were also analyzed to determine composition and to reveal if gallium is lost in the reaction. According to the chemical equation, the solid product should be some form of aluminum hydroxide. Theoretically, the gallium should not be consumed in the reaction, but realistically some gallium is likely to oxidize in the water. The white powdery substance described in Section 3.3 was collected, dried and then analyzed using XRD. The raw data of this analysis is shown in Figure 4.2.2. The analysis of the data indicates that both aluminum hydroxide and gallium oxide are present in the powder, however, the gallium oxide peaks are all

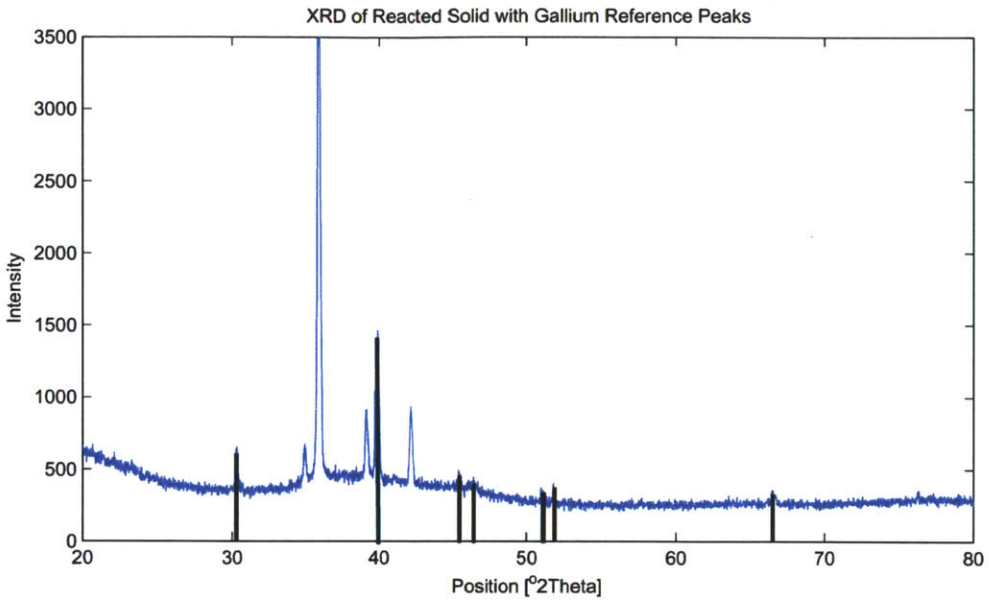

Figure 4.2.1: Plot of XRD data of the reacted metal. Gallium reference peaks are also plotted.

much less intense than the aluminum hydroxide peaks indicating that the aluminum hydroxide is dominant in the powder. Once again, more extensive crystallography must be done in order to determine exact composition of the reaction products.

4.2.2 Experimental Procedure

An experiment was designed in order to collect the hydrogen gas from the reaction. (Figure 4.2.3) A beaker is filled with water and a 100 mL graduated cylinder with 0.2 mL graduations is inverted full of water over the beaker such that the mouth is below the level of water in the beaker and no water escapes from the system. A syringe with liquid Ga-Al is weighed, and then a small amount is injected into an inverted funnel below the graduated cylinder. As the reaction proceeds, the funnel channels the hydrogen gas into the graduated cylinder, where it displaces the water back into the beaker. Because the whole system is open to the atmosphere, the pressure of

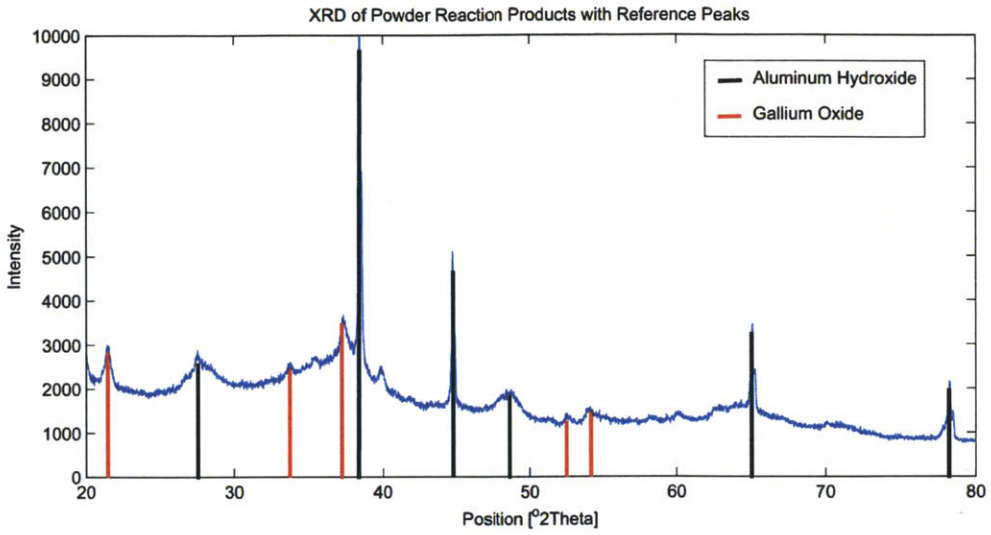

Figure 4.2.2: Plot of XRD data of the reaction products. Aluminum hydroxide and gallium oxide reference peaks are also plotted.

the hydrogen gas is approximately atmospheric pressure. The actual pressure of the hydrogen is $P_{atm} - \rho g \Delta h$, where Δh is the distance between the water level in the graduated cylinder and the water level in the beaker. Because Δh is relatively small in the experimental setup, the hydrogen pressure is approximated as atmospheric.

The syringe is weighed again after the injection of the metal into the setup, and the difference between the initial and final masses is taken to be the sample mass. Using Equation 4.2.1, the hydrogen yield is converted to aluminum mass reacted. Concentration is given by dividing the aluminum mass by the initial sample mass.

4.3 Determining Diffusion Rate and Saturation Concentration

In order to characterize the diffusion rate of aluminum into gallium as a function of aluminum concentration and temperature an experiment was designed to measure the diffusion rate. The diffusion rate is characterized in the same units as the reaction rate, that is $\frac{\text{mg}}{\text{cm}^2\text{s}}$, or mass of aluminum per surface area of aluminum per unit time.

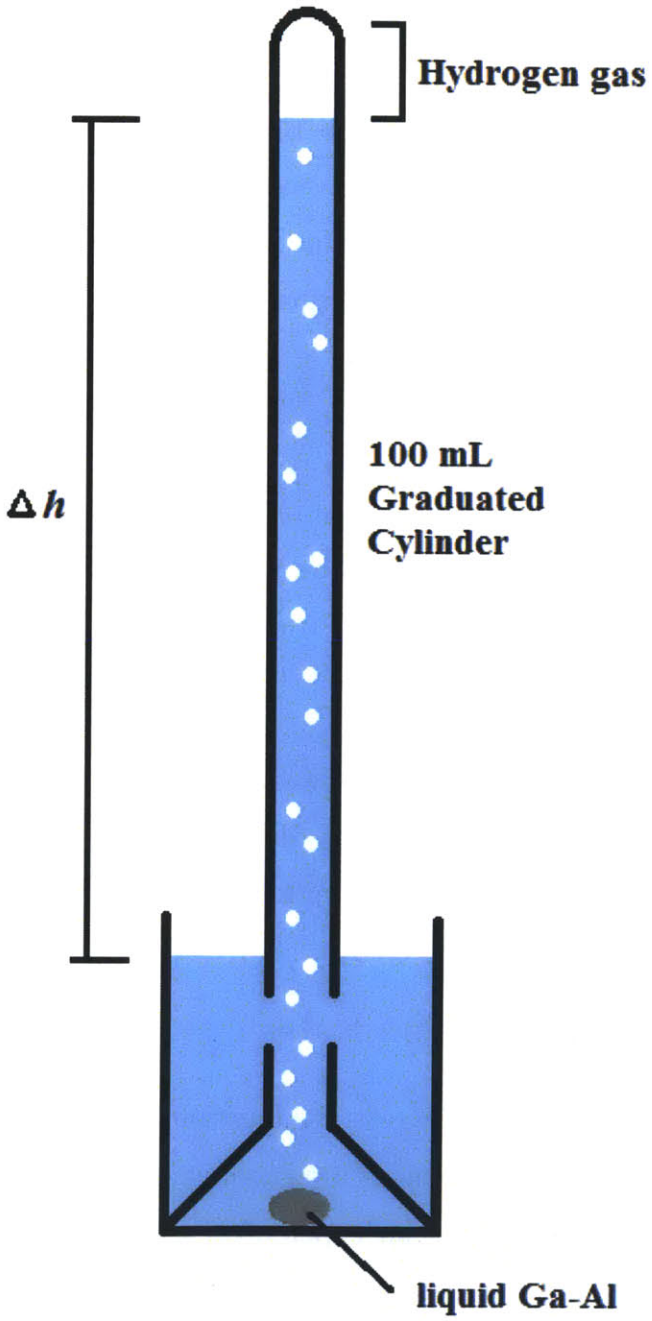

Figure 4.2.3: Experimental setup to react Al-Ga alloy and measure H_2 yield.

4.3.1 Inter-Diffusion Theory

The fundamental law of inter-diffusion is of the form

$$c_0 - c = Ae^{-k_{\text{diff}}t}, \tag{4.3.1}$$

where c_0 is the saturation concentration, c is the concentration at time t, A is a constant depending on the initial and final concentration and k_{diff} is a rate constant dependent upon the temperature at which diffusion takes place [11]. Differentiating this equation gives the diffusion rate as a function of time,

$$c'_{\text{diff}} = k_{\text{diff}}Ae^{-k_{\text{diff}}t}. \tag{4.3.2}$$

Combining the concentration equation and the rate concentration to eliminate time shows that the diffusion rate is theoretically linear with concentration,

$$c'_{\text{diff}} = k_{\text{diff}}(c_0 - c). \tag{4.3.3}$$

Because the saturation concentration can be determined experimentally and the rate is given by the linear function, given the initial diffusion rate at $c = 0$ the diffusion rate can be determined at all concentrations up to the saturation concentration.

4.3.2 Measuring the Diffusion Rate

The difficulty in measuring the diffusion rate as a function of concentration lies in the fact that the concentration measurement is a destructive process (the measurement reacts out all of the aluminum). So, an experiment was designed where a small amount of aluminum was completely diffused into a gallium bath held a constant temperature. The mass and surface area of the aluminum are known, and the time until the aluminum is completely dissolved is measured. The rate of this diffusion is taken to be the rate at $c = 0$. A large amount of aluminum is then submerged in the gallium bath and left for a long period of time until the gallium is assumed to be

Temperature (ºC)	90	130	160
Diffusion Rate, c'_{diff} ($\frac{mg}{cm^2 s}$)	0.0133	0.016	0.0266

Table 4.3.1: Diffusion rate, c'_{diff}, data at $c=0$.

saturated with aluminum. The saturation concentration is measured and the rate, c'_{diff}, at that concentration is assumed to be 0.

The experiment was conducted with three different beakers each with ≈15 mL gallium each covered with a layer of oil. The beakers were held at different temperatures (90º, 130º, 160º C) on a hotplate. Oil has a boiling point greater than 200º C, so it was used to prevent an oxide layer from forming on the gallium and allowed the gallium to reach relatively high temperatures. Small (1 cm^2) aluminum squares of 18 micron thickness were submerged in each beaker of gallium between two pieces of wire mesh. The aluminum samples were checked every few seconds and when the aluminum samples were no longer visible in any form, the time was recorded. A schematic of the setup is shown in Figure 4.3.1, and a picture of the setup is shown in Figure 4.3.2.

The diffusion rate is determined by dividing the aluminum mass by the surface area of the aluminum and the time to dissolve the aluminum. The results are summarized in Table 4.3.1.

4.3.3 Saturation Concentration of Aluminum in Liquid Gallium

The samples from the diffusion experiment, after being saturated, were reacted in order to measure the aluminum concentration. The data is shown in Table 4.3.2.

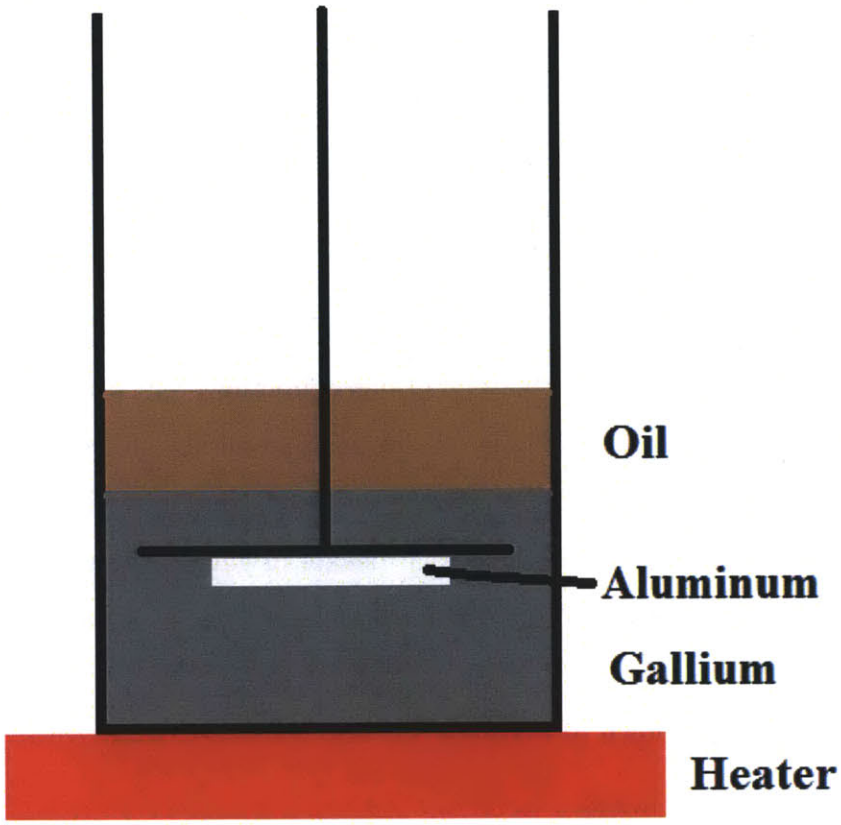

Figure 4.3.1: Schematic of diffusion rate experimental setup.

Trial	1	2	4	5	6	7	8	9
Reaction Temp	45	45	45	45	45	45	45	45
Diffusion Temp	90	90	130	130	130	160	160	160
Date	04/20/12	04/20/12	04/21/12	04/21/12	04/21/12	04/21/12	04/21/12	04/21/12
Before Weight (g)	15.278	11.097	29.233	27.021	23.819	25.227	21.800	16.579
After Weight (g)	11.235	8.262	27.271	23.819	20.968	21.876	16.579	14.220
Sample Mass (g)	4.043	2.835	1.962	3.202	2.851	3.351	5.221	2.359
Approx. Surface Area (cm^2)	3.728	2.939	2.299	3.188	2.951	3.287	4.417	2.600
mL H_2	52.400	42.000	29.600	48.000	40.600	48.600	76.600	36.000
g Al	0.0422	0.0338	0.0238	0.0386	0.0327	0.0391	0.0616	0.0290
% Al	1.043	1.192	1.214	1.206	1.146	1.167	1.180	1.228

Table 4.3.2: Aluminum saturation concentration data for select samples of different diffusion temperatures.

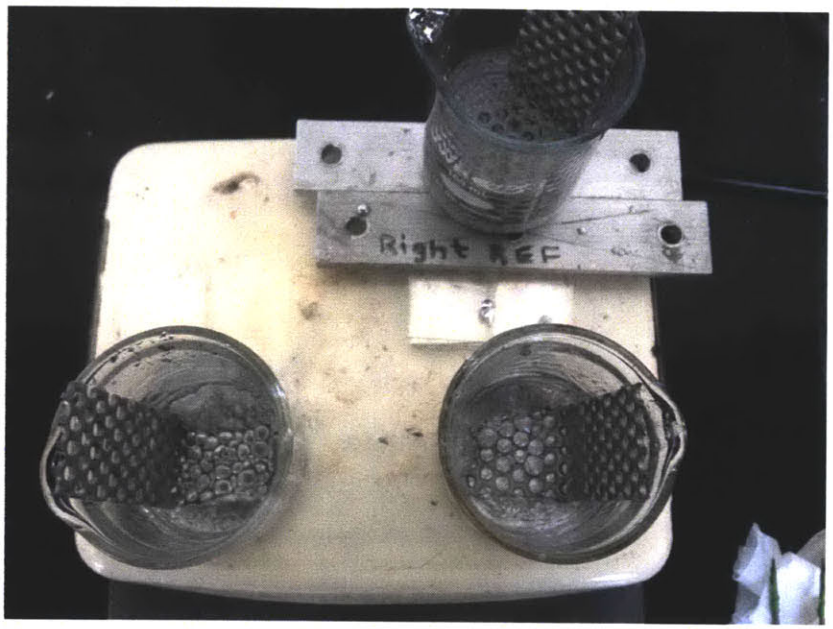

Figure 4.3.2: Photo of diffusion rate experimental setup. Steel mesh is used to prevent the aluminum from floating to the surface of the liquid gallium.

The data indicates that the diffusion temperature has no effect on the saturation concentration. From the data, the saturation concentration of aluminum in liquid gallium, c_0, is 1.17 $\pm$0.05 wt%.

4.3.4 Diffusion Rate Results

The initial diffusion rate and the saturation concentration can be used to determine the concentration and temperature dependence of aluminum diffusion into gallium. The diffusion rate $c'_{\text{diff}}(0)$ is given in Table 4.1. The diffusion rate at the saturation concentration is zero, so that $c'_{\text{diff}}(c_0)= 0$, where c_0 is the saturation concentration given in Table 4.2. Applying these parameters to Equation 4.3.3, the rate constant k_{diff} can be determined. The results are plotted to show the diffusion rate dependence on concentration at the three experimental temperatures. (Figure 4.3.3)

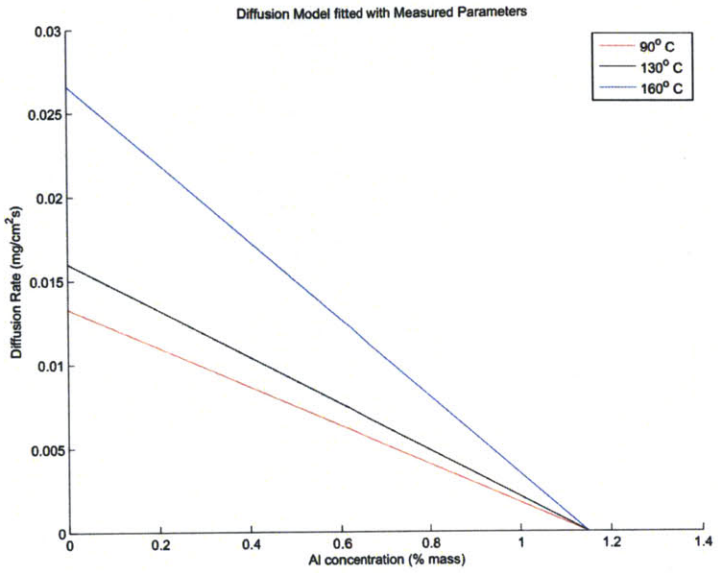

Figure 4.3.3: Diffusion rate as a function of concentration, c, at multiple temperatures. The slope of the lines give the temperature dependent rate constant, k_{diff}.

4.3.5 Temperature Dependence of Diffusion Rate Constant

The diffusion rate constant, k_{diff}, is described with the Arrhenius equation,

$$k = Ae^{-E_a/RT}, \tag{4.3.4}$$

where T is the temperature of diffusion (in Kelvin), E_a is the activation energy ($\frac{\text{J}}{\text{mol}}$), R is the universal gas constant ($\frac{\text{J}}{\text{mol}\cdot\text{K}}$) and A is the theoretical maximum diffusion rate if T were infinite ($\frac{\text{mg}}{\text{cm}^2\text{s}}$). The Arrhenius equation is rearranged to the slope-intercept form

$$ln(k) = \frac{\alpha}{T} + \beta, \tag{4.3.5}$$

such that the diffusion data from Figure 4.3.3 can be plotted to determine the constants α and β from a linear fit. By plotting the natural log of the empirically determined diffusion rate constant k_{diff} against the inverse of the diffusion temperature, T, the data should fall on a line. The constant A and the activation energy E_a are then given by

$$A = e^{\beta} \tag{4.3.6}$$

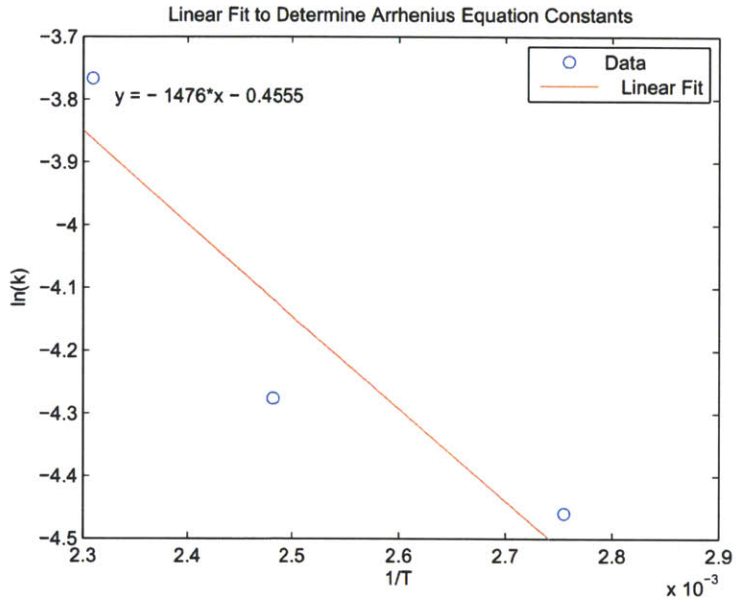

Figure 4.3.4: Linear fit of diffusion rate data to determine Arrhenius constant and activation energy.

and

$$E_a = -\alpha R. \tag{4.3.7}$$

The three diffusion rate constants from Figure 4.3.3 are plotted and fit with a linear function in order to determine the α and β constants given in Equation 4.3.5. (Figure 4.3.4)

The constants from the linear fit of the diffusion rate data in Figure 4.3.4 give an activation energy of diffusion for aluminum into gallium of $E_a = 12.3\ \frac{\text{kJ}}{\text{mol}}$ and a pre-exponential constant of $A = 0.634\ \frac{\text{mg}}{\text{cm}^2\text{s}}$. Plugging these constants into the Arrhenius equation yields the experimentally determined diffusion rate function for aluminum in liquid gallium,

$$k_{\text{diff}}(T) = 0.634e^{-12.3e3/RT}. \tag{4.3.8}$$

Plotting Equation 4.3.8 over a larger range of temperature gives a rough approximation of the diffusion rate constant as a function of temperature. (Figure 4.3.5)

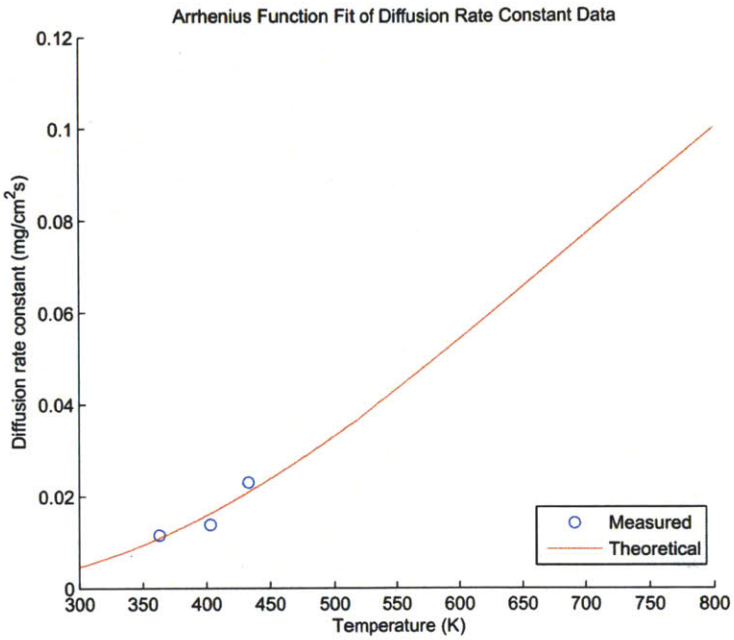

Figure 4.3.5: Predicted diffusion rate constant at increased temperatures.

4.4 Measuring Reaction Rate

4.4.1 Concentration Dependence of Reaction Rate

In order to determine how the reaction rate is a function of aluminum concentration, the hydrogen level in the graduated cylinder is tracked over time by videotaping the hydrogen accumulation in the graduated cylinder. The video is analyzed and the position of the meniscus is tracked as a function of time. Using Equation 4.2.1 and the mass of each reacted sample, a normalized aluminum concentration (wt%) can be plotted with respect to time. The experiment was conducted at different system temperatures in order to determine the temperature dependence of the reaction rate constant. Samples on the order of 2 grams were tested in water temperatures of 45^{o}, 60^{o}, and 80^{o} C. The raw data from the video analysis is shown in Figure 4.4.1.

In order to determine the rate of the reaction, the aluminum content as a function of time is normalized to surface area and differentiated with respect to time to give the desired units of $(\frac{mg}{cm^2 s})$. The surface area of the reacting liquid metal is calculated using the mass of the sample, the density of the sample and the number of discrete

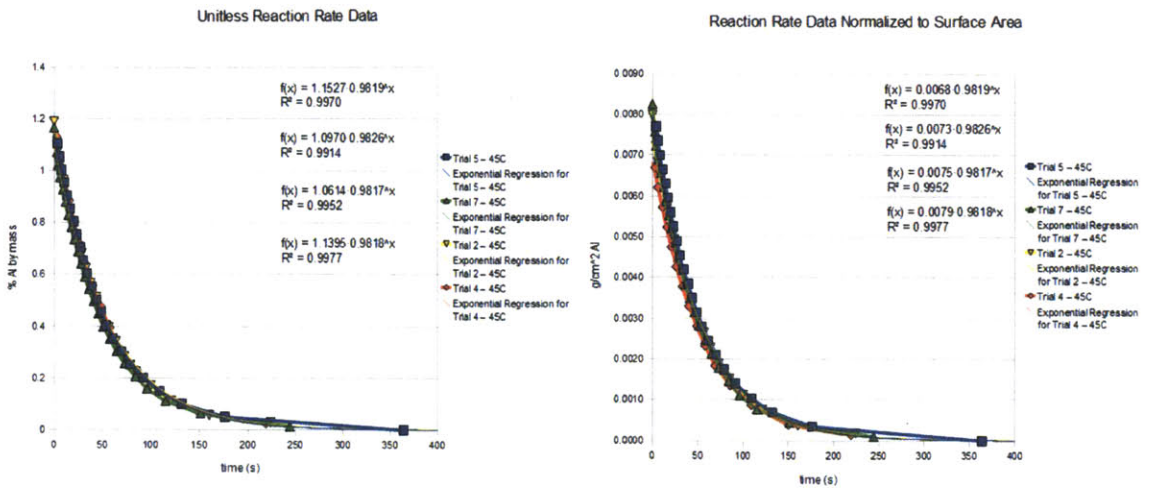

Figure 4.4.1: Raw data of aluminum concentration as a function of time when Ga-Al is dropped in water. Aluminum concentration is calculated from hydrogen yield. Left plot shows aluminum concentration in wt%. Right plot shows aluminum concentration normalized to surface area.

drops that the liquid metal formed in the water. The drops are approximated as spherical. The resulting surface area of the reacting liquid is given by

$$SA_{sample} = 4\pi n\left(\frac{3}{4\pi}\frac{(m_{sample} - m_{\mathrm{Al}})}{n\rho_{Ga}}\right)^{2/3} \tag{4.4.1}$$

where n is the number of drops, m_{sample} is the original mass of the sample, m_{Al} is the mass of aluminum reacted and ρ_{Ga} is the density of gallium, 5.9 $\frac{\mathrm{g}}{\mathrm{mL}}$.

Because the data itself cannot be differentiated, exponential curves are fit to both the unitless data and the data normalized to surface area to give functions

$$\mathrm{wt\%}(t) = A \cdot B^t \tag{4.4.2}$$

and

$$\frac{\mathrm{m}}{\mathrm{SA}}(t) = C \cdot D^t. \tag{4.4.3}$$

The exponential fit for the mass normalized to surface area (Equation 4.4.3) is differentiated with respect to time to give the reaction rate. The resulting reaction rate ($\frac{\mathrm{mg}}{\mathrm{cm^2 s}}$) as a function of time is plotted parametrically against the aluminum concentration (Equation 4.4.2) to give the reaction rate as a function of concentration at

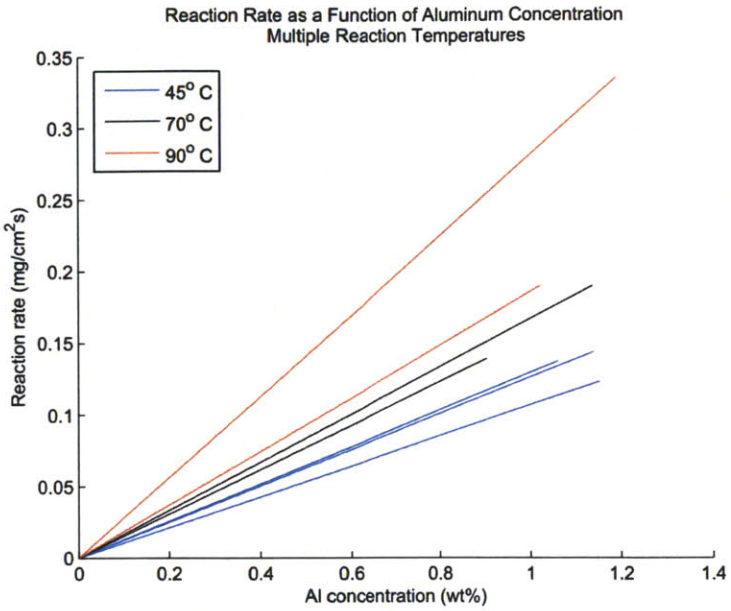

Figure 4.4.2: Reaction rate ($\frac{\text{mg}}{\text{cm}^2\text{s}}$) as a function of aluminum concentration and temperature.

multiple temperatures. (Figure 4.4.2)

For an exponential fit of the data, the reaction rate is positively linear with the aluminum concentration in the gallium. This is the expected correlation of a first-order reaction, where the reaction rate is given by

$$c'_{\text{rxn}} = k_{\text{rxn}}(T) \cdot c \tag{4.4.4}$$

where c is the concentration of the reactant and $k_{\text{rxn}}(T)$ is the reaction rate constant. The data also shows that as the temperature of the reaction increases, the reaction rate constant also increases, which is expected for a reaction rate constant that follows the Arrhenius equation.

4.4.2 Reaction Rate Constant

Because the reaction rate constant, $k_{\text{rxn}}(T)$, is also described by the Arrhenius equation, the technique described in section 4.3.5 is the same technique used to determine the reaction rate constant from the experimental data.

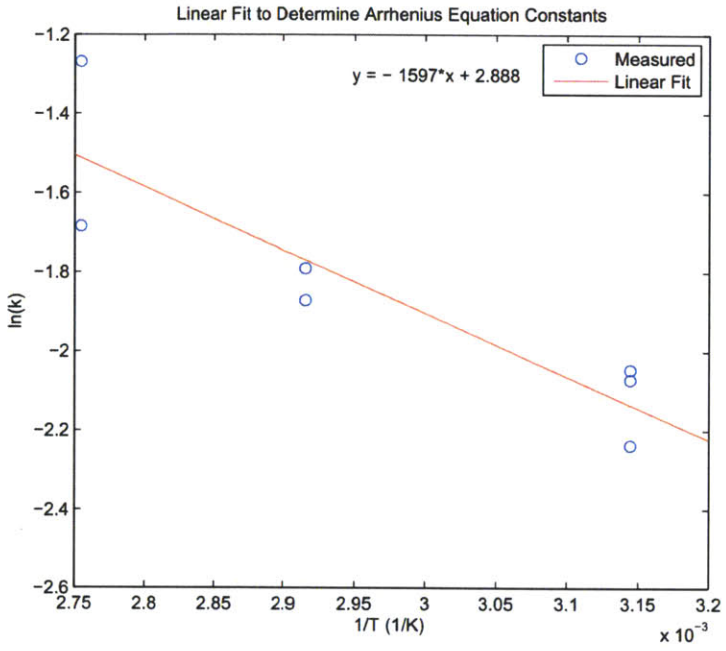

Figure 4.4.3: Linear fit of reaction rate data to determine Arrhenius constant and activation energy.

The natural log of the reaction rate constants from Figure 4.4.2 are plotted against the inverse of the temperature and fit with a linear function. (Figure 4.4.3)

The constants from the linear fit of the reaction rate data give an activation energy of reaction of $E_a = 13.3 \frac{\text{KJ}}{\text{mol}}$ and a pre-exponential constant of $A = 17.87 \frac{\text{mg}}{\text{cm}^2\text{s}}$. Plugging these constants into the Arrhenius equation yields the experimentally determined reaction rate function for aluminum reacting from liquid gallium,

$$k_{\text{rxn}}(T) = 17.87e^{-13.3\times10^3/RT}. \tag{4.4.5}$$

Plotting this function over a larger range of temperature gives a rough approximation of the reaction rate constant as a function of temperature. (Figure 4.4.4)

4.5 Homogeneity of the Liquid Alloy

One of the assumptions in the modeling of the system is that the concentration of aluminum in the gallium is spatially uniform. In order to validate this assumption, an

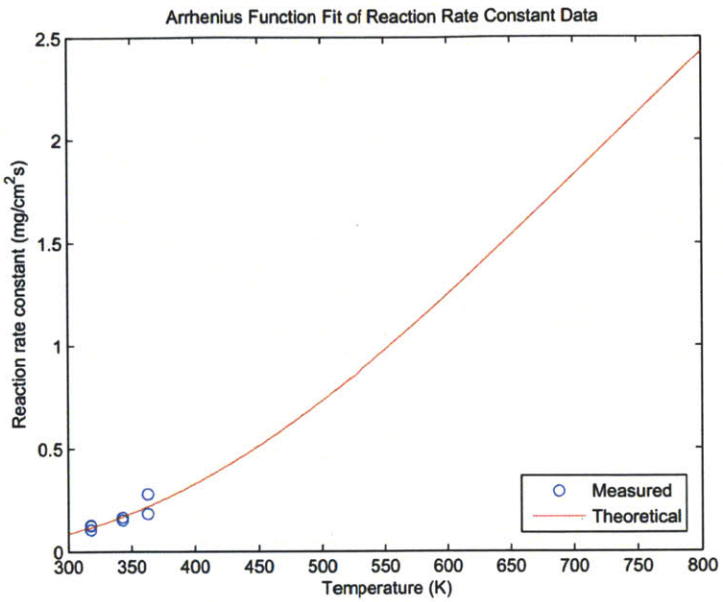

Figure 4.4.4: Predicted reaction rate constant at increased temperatures.

experiment was designed to give reasonable evidence that the assumption is correct. A syringe with a ball of aluminum wire at one end was filled with liquid gallium and held at room temperature such that the gallium remained liquid. A diagram of the setup is shown in Figure 4.5.1. The experiment relies on the fact that the liquid gallium is static and that diffusion is happening at one end of the long slug of gallium such that if the diffusion rate inside the gallium was small, a concentration gradient would appear along the length of the syringe.

After 90 minutes, the gallium was pushed out of the syringe in segments and reacted, such that each sample reacted is a different distance from the diffusion interface and any concentration gradients would be apparent. The hydrogen gas was collected from the reacted samples and used to determine the aluminum concentration in the gallium. The results from the experiment are shown in Table 4.5.1.

The experiment is validated by the fact that the aluminum concentration had not yet reached saturation, which is indication that there was still a significant diffusion flux between the aluminum and gallium. For three samples, each 1 cm apart, the aluminum concentration was the same within the error of the measurements. This proves that the aluminum-gallium solution can be considered homogenous. This

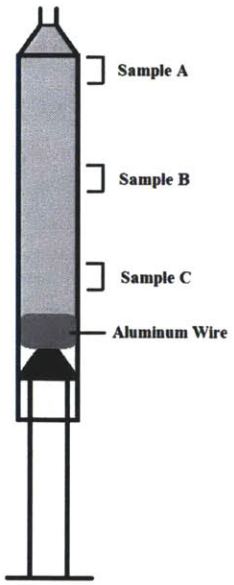

Figure 4.5.1: Schematic of experimental setup used to determine spatial distribution of aluminum in liquid gallium.

Sample	Distance from Al (cm)	Reacted Mass (g)	Hydrogen Yield (mL)	Al content (wt%)
A	3	2.67	0.8 mL	0.27
B	2	2.64	0.8 mL	0.27
C	1	2.25	0.8 mL	0.23

Table 4.5.1: Data from homogeneity experiment.

homogeneity is most likely because the rate at which aluminum atoms move inside the liquid gallium is much faster than the rate at which aluminum atoms are removed from the solid aluminum.

4.6 Ga-In-Sn as a Diffusion Metal

Previous work with solid phase alloys have revolved around a eutectic composition of Ga, In and Sn (68 wt% Ga, 22 wt% In, 10 wt% Sn) because of the extremely low melting temperature of the metal (-19^{o} C) [7]. The low melting temperature helps drive down the melting point of the resulting Al-Ga-In-Sn alloy, which is advantageous for the reaction activation. However, previous work did not investigate the diffusion properties of the Ga-In-Sn alloy, an important part of the approach outlined in this

thesis. A diffusion and reaction experiment was conducted in order to understand how the diffusion and reaction of aluminum would proceed in liquid phase Ga-In-Sn.

Approximately 0.4 g of aluminum wire was inserted into a syringe of approximately 2.5 mL of liquid metal. The syringe was left to diffuse at room temperature for 48 hours. The same experiment was set up with pure gallium as the liquid metal as a control. After the 48 hours, the solid remnants of the wire were removed, and samples of the liquid alloy were dropped into warm water and the hydrogen gas produced from the reaction was collected as before. The results of the experiment are shown in Table 4.6.1.

Material	Reacted Mass (g)	Hydrogen Yield (mL)	Al Content (wt%)	Reaction Time (min)
Ga-In-Sn	1.57	3.2	0.16	90
Ga-In-Sn	1.32	6.0	0.36	120
Ga	3.37	38.0	0.9	20
Ga	2.0	30.0	1.2	20
Ga	3.48	45.0	1.0	20

Table 4.6.1: Results of Ga-In-Sn diffusion and reaction experiment with a Ga control.

The results indicate two important pieces of information. First, the saturation concentration of Al in Ga-In-Sn is less than the saturation concentration of Al in Ga by approximately a factor of 3. Second, the reaction time of the Al in the Ga-In-Sn alloy is considerably longer than the reaction time of Al in Ga, showing that the reaction rate of Al in Ga-In-Sn is slower than the reaction rate of Al in Ga.

A possible explanation for this result is that the Ga-In-Sn alloy has bigger In and Sn atoms dispersed throughout. The larger atoms leave less unoccupied space for the aluminum atoms to occupy, which results in the lower saturation concentration. The larger In and Sn atoms also act as barricades for the aluminum atoms to move around the solution, resulting in slower diffusion within the liquid and slower reaction rates because it takes longer for the aluminum atoms to reach the water interface.

Chapter 5

Constraining the Reactor Design Criteria

The work in Chapter 4 attempts to characterize the reaction and diffusion rates of aluminum in liquid metal in order to predict reactor performance at higher temperatures. Because the diffusion and reaction rates are given as a flux, the mass transfer rates of aluminum into and out of the liquid metal can be equated by appropriate design of the diffusion and reaction surface areas in a reactor.

In order to realize a working reactor based on the in-situ diffusion approach discussed in Chapter 3, the surface area of diffusion must be related to the surface area of reaction as a function of temperature and aluminum concentration in gallium. By relating these variables, the design space is constrained around the stable operating point of the reactor.

5.1 Reaction Rate

The reaction rate of the aluminum with the water is a function of the aluminum concentration and the temperature of the reaction. Experiments have shown that the reaction rate is linear with the concentration, and follow the equation $c'_{\text{rxn}} = k_{\text{rxn}}(T) \cdot c$. The units of c'_{rxn} in this paper are $(\frac{\text{mg}}{\text{cm}^2\text{s}})$. The reaction rate is directly proportional

to the power output of the reaction, such that

$$P = c'_{\text{rxn}} SA_{\text{rxn}} U_{\text{Al}}, \tag{5.1.1}$$

where SA_{rxn} is the reaction surface area and U_{Al} is the heat energy released per unit mass of Al reacted. Thus,

$$P = k_{\text{rxn}}(T) \cdot c \cdot SA_{\text{rxn}} \cdot U_{\text{Al}}, \tag{5.1.2}$$

so in order to maximize the power output of the reaction, the temperature and concentration should be maximized. This indicates that the size of the reactor doesn't necessary correspond to the power output of the reactor and proves that a small reactor can have a greater power output just by increasing the temperature and aluminum concentration in the gallium.

5.2 Diffusion Rate

The diffusion rate of the aluminum into the gallium is a function of the aluminum concentration and the temperature. Experiments have confirmed that diffusion rate is inversely linear with concentration, and follows the equation $c'_{\text{diff}} = k_{\text{diff}}(T)(c_0 - c)$, where $k_{\text{diff}}(T)$ is given by Equation 4.3.8.

5.3 Relating Surface Area

In order for the reaction to be sustained at the desired rate, the mass flow rate of aluminum into the gallium must be equal to the mass flow rate of aluminum reacting out of the gallium. The concentration of the aluminum in the gallium will settle to the natural amount where these two rates are equal, but in order to maximize power output, the ratio of the surface areas can be designed such that the reactor operates at a desired aluminum concentration.

The following equation is given from the conservation of energy in the reactor:

$$c'_{\text{diff}} \cdot SA_{\text{diff}} = c'_{\text{rxn}} \cdot SA_{\text{rxn}}. \tag{5.3.1}$$

Combining Equation 5.3.1 with Equations 4.3.3 and 4.4.4 gives the relation

$$\frac{SA_{\text{diff}}}{SA_{\text{rxn}}} = \frac{k_{\text{rxn}}(T) \cdot c}{k_{\text{diff}}(T)(c_0 - c)} \tag{5.3.2}$$

which relates the diffusion and reaction area to the temperature and aluminum concentration in the reactor.

Plotting Equation 5.3.2 with the experimental values of $k_{\text{rxn}}(80°C)$ and $k_{\text{diff}}(80°C)$ for $c = 0$ to 1.15 wt% gives the required surface area ratio as a function of aluminum concentration for a reactor operating at 80^{o} C. As the aluminum concentration approaches the saturation concentration, the required diffusion surface area becomes much larger than the reaction surface area. (Figure 5.3.1)

In order to also understand the temperature dependence of the surface area ratio, the surface area ratio is calculated as a function of both the aluminum concentration and the temperature. The experimentally-determined temperature dependencies of the diffusion and reaction rate constants, Equations 4.3.8 and 4.4.5, are substituted into Equation 5.3.2. The surface plot of the resulting equation is shown in Figure 5.3.2 with the near-saturation concentrations omitted in order to eliminate the unrealistic surface area ratios.

The plot in Figure 5.3.2 indicates that the surface area ratio is almost entirely dependent on the aluminum concentration in the gallium and is only weakly dependent on the reaction temperature.

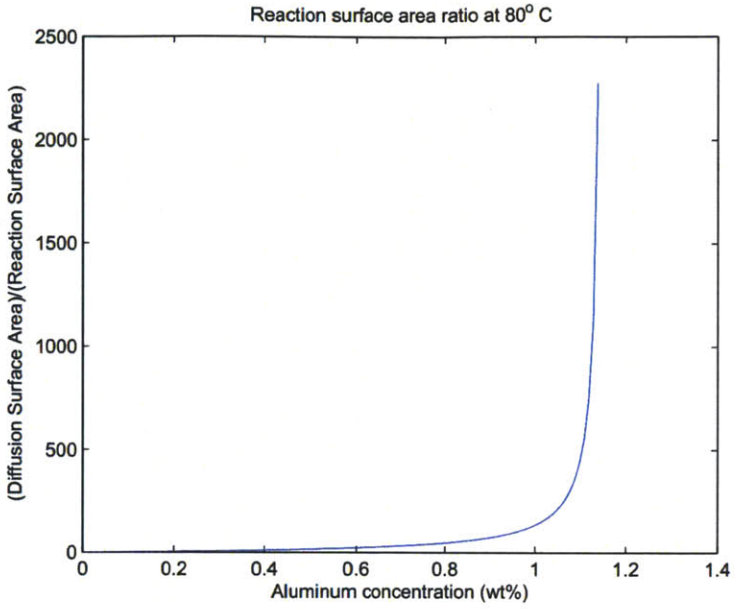

Figure 5.3.1: Required surface area ratio as a function of steady state aluminum concentration. Plot is generated from measured diffusion and reaction rates.

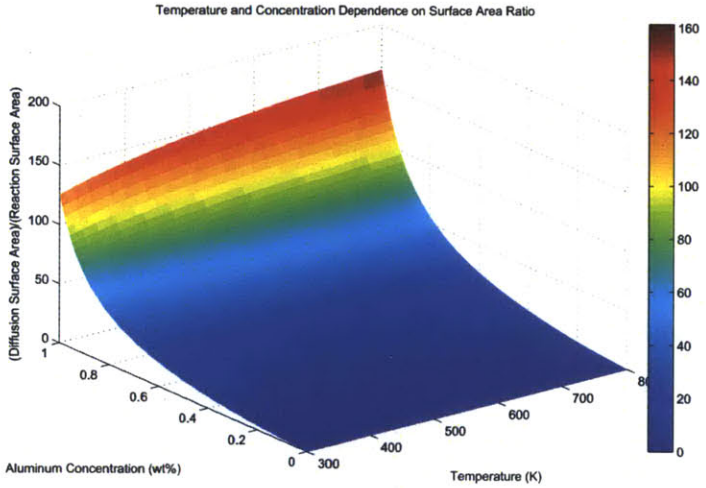

Figure 5.3.2: Temperature and concentration dependence of the surface area ratio in an interdiffusion-based aluminum-water reactor.

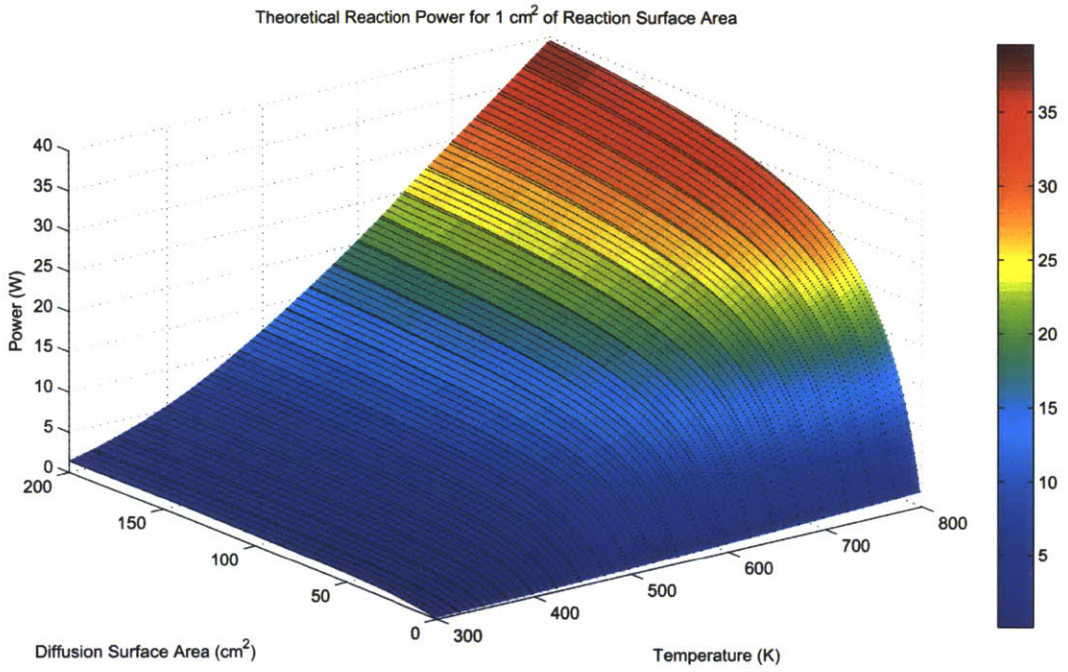

Figure 5.4.1: Predicted reaction power for variable reactor parameters at 1 cm^2 of reaction surface area.

5.4 Theoretical Reaction Power Output

A more useful result than of that shown in Figure 5.3.2 is the reaction power output as a function of the reactor design parameters, specifically the temperature, diffusion and reaction surface areas. Combining Equations 5.1.2 and 5.3.2 gives the power output as a function of the named parameters

$$P = U_{\mathrm{Al}} k_{\mathrm{rxn}}(T) SA_{\mathrm{diff}} \left(\frac{k_{\mathrm{diff}}(T) c_0}{k_{\mathrm{rxn}}(T) + \frac{SA_{\mathrm{diff}}}{SA_{\mathrm{rxn}}} k_{\mathrm{diff}}(T)} \right). \tag{5.4.1}$$

A plot of Equation 5.4.1 at a constant reaction surface area of 1 cm^2 is shown in Figure 5.4.1. Expanding the plot to larger power outputs, a plot of Equation 5.4.1 at a constant reaction surface area of 25 cm^2 is shown in Figure 5.4.2.

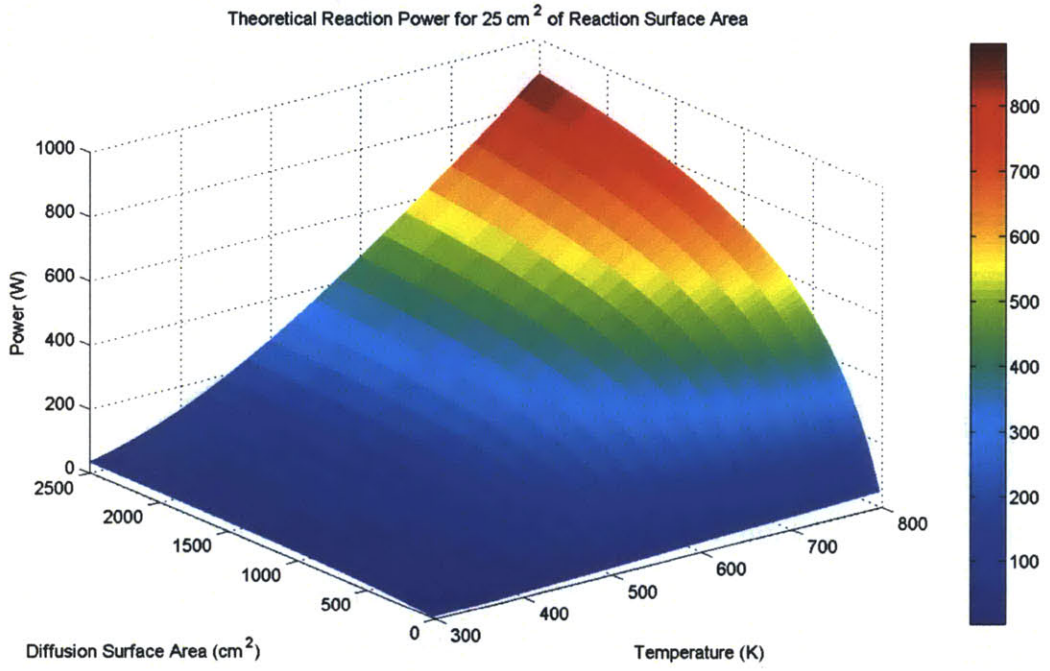

Figure 5.4.2: Predicted reaction power for variable reactor parameters at 25 cm^2 of reaction surface area.

Chapter 6

Discussion and Future Work

By measuring the rate of reaction and the rate of diffusion at different temperatures, as well as the saturation concentration of aluminum in gallium, the reaction rate constant, $k_{\text{rxn}}(T)$, and diffusion rate constant, $k_{\text{diff}}(T)$, were determined by fitting the data to the Arrhenius equation. The two constants are combined with the concentration dependence of the reaction and diffusion rates to predict the rate of reaction and the rate of diffusion at any temperature and concentration. The reaction and diffusion rates are related by the conservation of mass and combined with the thermodynamics of the reaction to give a predicted power output of the reaction for different reactor design parameters.

The predicted power output of the reaction shown in Figure 5.4.1 and 5.4.2 is a rough approximation based on the experiments conducted in this thesis. With more data and improved methods, the reaction rate and diffusion rate constants could be refined even further. It is predicted that the reaction rate constant and diffusion rate constant are also a function of many other system variables, and future models would explore these variables and their effect on the rate constants.

6.1 Discussion of Results

The predicted power output from Chapter 5 gives a rough idea of the size and temperature required of a prototype reactor. The power output from the reaction can

be multiplied by the system efficiency for a prototype heat engine system to estimate the total system power output. The results indicate that a reactor operating at 500 K with 25 cm^2 of reaction surface area and 900 cm^2 of diffusion surface area could output roughly 20 W with a total system efficiency of 10%. The same system operating at 700 K would output roughly 50 W of power. This size of a reactor is nearly large enough to power an AUV such as the REMUS 600.

While more data should be taken to verify the diffusion and reaction rates, the results in this thesis confirm the dependencies on temperature and aluminum concentration and give a reasonable estimate of how an in-situ interdiffusion aluminum-water reaction will perform.

6.2 Future Work

In order to better understand the processes occurring in the in-situ interdiffusion aluminum-water reaction, more experiments should be conducted in which other system variables are varied. A prototype reactor should also be built such that the predictions made in this thesis can be experimentally verified.

6.2.1 System Pressure

A reactor operating above 100^{o} C must operate at a pressure greater than atmospheric in order to maintain the water in the liquid phase. While the reaction would proceed with water vapor, the reaction products would not be able to suspend in the liquid water so it is possible that they would interfere with the reaction. Because an elevated pressure is desired for the reactor operation, the reactor will be more efficient at depth than at the surface because less power will be used to pressurize the water. At 200 meters depth, the reactor could operate in liquid phase at temperatures up to 210^{o} C before additional power is required to pressurize the water.

The rate constants are theoretically dependent on the pressure, so further work should be conducted to measure the pressure dependence. A pressurized reaction setup would have the additional advantage of measuring the reaction rate at higher

temperatures. With the current setup used in this thesis, the temperature is limited by the boiling point of the water; if the water boils, water vapor rises into the graduated cylinder and has a significant contribution to the gas volume, making it impossible to know how much hydrogen is produced.

6.2.2 Other System Variables

There are many system variables that were held constant in this thesis but could be varied to determine their effects on the parameters that were determined experimentally. Water salinity, aluminum composition and crystal structure and gallium additives are predicted to all have an effect on the reaction and diffusion rate constants. It is expected that these parameters will have smaller effects on the system performance compared to the major parameters of aluminum concentration and temperature.

Bibliography

[1] Rutgers University. *Flight Across the Atlantic - Scarlet Knight.* (2009, December 12). Retrieved from http://rucool.marine.rutgers.edu/atlantic/. Accessed May 21, 2012.

[2] MIT Rapid Development Group: 2.013 Engineering Systems Design. *Internal Combustion Engine Hybrid Recharging System.* (2012). Informally published manuscript, Department of Mechanical Engineering, Massachusetts Institute of Technology, Cambridge, MA.

[3] Monterey Bay Aquarium Research Institute (MBARI). (2010, August 17). *AUV: Docking System.* Retrieved from http://www.mbari.org/auv/dockingvehicle.htm. Accessed May 21, 2012.

[4] Autonomous Undersea Systems Institute (AUSI). *Research: Solar AUV (SAUV).* Retrieved from http://ausi.org/research/sauv. Accessed May 21, 2012.

[5] U.S. Department of Energy. (2008). *Reaction of Aluminum with Water to Produce Hydrogen: A Study of Issues Related to the Use of Aluminum for On-Board Vehicular Hydrogen Storage.* Retrieved September 25, 2011, from http://www1.eere.energy.gov/hydrogenandfuelcells/pdfs/aluminium_water_hydrogen.pdf

[6] Miller, T. F., & Walter, J.L., & Kiely, D.H. (2002). A Next-Generation AUV Energy System Based on Aluminum-Seawater Combustion. *Proceedings of the 2002 Workshop on Autonomous Underwater Vehicles, 2002,* 111-119. doi:10.1109/AUV.2002.1177213

[7] Ziebarth, Jeffrey T. (2010). *Use of the Al-Ga-In-Sn System for Energy Storage and Conversion.* (Doctoral dissertation, Purdue University). (Publication No. AAT 3417965)

[8] Techshot, Inc. *AlGalCo Case Study.* Retrieved from http://www.techshot.com/case-studies.aspx/algalco. Accessed May 5, 2012.

[9] Begg, Alan. (1984). *U.S. Patent 4,501,611.* Washington, DC: U.S. Patent and Trademark Office.

[10] HighScore Plus (Version 3.0) [Software]. (2012). The Netherlands: PANalytical B.V.

[11] Owen, E. A., & Pickup, L. (1932). *Inter-Diffusion of Metals. Nature, 130,* 201-202.